Biochemical characterization, distribution and phylogenetic analysis of *Drosophila melanogaster* ryanodine and IP_3 receptors, and thapsigargin-sensitive Ca^{2+} ATPase

Olivia Vázquez-Martínez[1], Rafael Cañedo-Merino[1], Mauricio Díaz-Muñoz[1,*] and Juan R. Riesgo-Escovar[2,*]

[1]Department of Molecular and Cellular Neurobiology and [2]Department of Developmental Neurobiology and Neurophysiology, Neurobiology Institute, Campus UNAM-Juriquilla, Universidad Nacional Autónoma de México, Querétaro 76230, Mexico

*Authors for correspondence (e-mail: juan@zool.unizh.ch; mdiaz@calli.inb.unam.mx)

Accepted 5 March 2003
Journal of Cell Science 116, 2483-2494 © 2003 The Company of Biologists Ltd
doi:10.1242/jcs.00455

Summary

We characterized the biochemistry, distribution and phylogeny of *Drosophila* ryanodine (RyR) and inositol triphosphate (IP_3R) receptors and the endoplasmic reticulum Ca^{2+}-ATPase (SERCA) by using binding and enzymatic assays, confocal microscopy and amino acid sequence analysis. [^{3}H]-ryanodine binding in total membranes was enhanced by AMP-PCP, caffeine and xanthine, whereas Mg^{2+}, Ruthenium Red and dantrolene were inhibitors. [^{3}H]-ryanodine binding showed a bell-shaped curve with increasing free [Ca^{2+}], without complete inhibition at millimolar levels of [Ca^{2+}]. [^{3}H]-IP_3 binding was inhibited by heparin, 2-APB and xestospongin C. Microsomal Ca^{2+}-ATPase activity was inhibited by thapsigargin. Confocal microscopy demonstrated abundant expression of ryanodine and inositol triphosphate receptors and abundant Ca^{2+}-ATPase in *Drosophila* embryos and adults. Ryanodine receptor was expressed mainly in the digestive tract and parts of the nervous system. Maximum parsimony and Neighbour Joining were used to generate a phylogenetic classification of *Drosophila* ryanodine and insitol triphosphate receptors and Ca^{2+}-ATPase based on 48 invertebrate and vertebrate complete sequences. The consensus trees indicated that *Drosophila* proteins grouped with proteins from other invertebrates, separately from vertebrate counterparts.

Despite evolutionary distances, our functional results demonstrate that *Drosophila* ryanodine and inositol triphosphate receptors and Ca^{2+}-ATPase are reasonably similar to vertebrate counterparts. Our protein expression data are consistent with the known functions of these proteins in the *Drosophila* digestive tract and nervous system. Overall, results show *Drosophila* as a valuable tool for intracellular Ca^{2+} dynamics studies in eukaryotes.

Key words: Calcium release channel, Intracellular calcium, Sequence analysis, Confocal microscopy, *Drosophila*

Introduction

Intracellular Ca^{2+} dynamics is a key factor in cellular signaling and physiology (for a review, see Bootman et al., 2001). In particular, the system of endomembranes that forms the sarco(endo)plasmic reticulum plays a vital role in Ca^{2+} handling in most eukaryots (Carafoli and Klee, 1999). In this compartment two families of intracellular Ca^{2+} release channels have been characterized: the ryanodine receptors (RyR) and the inositol 1,4,5-trisphosphate receptors (IP_3R) (Nori et al., 1993). Besides these, there is evidence for two more intracellular Ca^{2+} releasing channels: the NAAPD and the sphingolipid receptors (Petersen and Cancela, 1999; Cancela, 2001). Ca^{2+} re-uptake by the sarco(endo)plasmic reticulum is mediated by the thapsigargin-sensitive sarco(endo)plasmic reticulum Ca^{2+} ATPase (SERCA), whose structure and function has been studied extensively in mammalian muscle systems (MacLennan, 1990).

The development of the fruit fly *Drosophila melanogaster* is amenable to multidisciplinary analyses (for a review, see Campos-Ortega and Hartenstein, 1997) and is thus a powerful system in which to examine the role of these proteins in intracellular Ca^{2+} homeostasis. In this organism, a single RyR gene with 26 exons, *dry*, and a single IP_3R gene with 12 exons, *dip*, exist and have been genetically characterized (Takeshima et al., 1994; Sinha and Hasan, 1999). In contrast, RyR and IP_3R in vertebrates are coded by at least three different genes that, due to alternative splicing, present a large number of isoforms (Rubtsov and Batrukova, 1997; Marks, 1997). A similar situation occurs with the thapsigargin-sensitive Ca^{2+} ATPase. In *D. melanogaster* only one gene coding for this P-type ATPase has been detected, *CaP60A* (Magyar et al., 1995); whereas in vertebrates, at least three different isoforms of this Ca^{2+} ATPase have been reported (Misquitta et al., 1999).

Despite extensive genetic and molecular biology data for these proteins, there is a dearth of basic biochemical information on the *Drosophila* RyR, IP_3R and SERCA proteins. In order to reap the benefit from a genetic and molecular biology tractable model organism with single RyR, IP_3R and SERCA proteins, we characterize here these important molecules using *Drosophila* native endomembranes.

(1) To characterize the proteins biochemically and pharmacologically we performed radioligand-binding assays for the *Drosophila* ryanodine and IP_3 receptors, and a coupled enzymatic determination for the thapsigargin-sensitive Ca^{2+} ATPase. These studies used subcellular fractions of native membranes of this insect, allowing us to compare the biochemical properties of these *Drosophila* proteins with their vertebrate homologs.

(2) We complemented these data with a detailed evaluation of the anatomical localization of these proteins in embryos and adults using fluorescent probes, confocal microscopy and image analysis. In particular, we noted widespread and high levels of expression and co-expression in the digestive tract.

(3) We performed a comprehensive comparison of the amino acid sequences of the two calcium release channels and the endoplasmic reticulum Ca^{2+} pump from *D. melanogaster* with similar proteins from other species. Our results show that these *Drosophila* proteins share many characteristics with their vertebrate cognates. However, differences in [^{3}H]-ryanodine binding and SERCA activity compared with vertebrate isoforms, imply also unique properties of the *Drosophila* RyR and SERCA.

Materials and Methods

Drosophila stocks

Wild type Oregon R (WT) and mutant *yellow white* (lighter cuticle color and white-eyed) (YW) stocks of *D. melanogaster* were used for the experiments. YW flies were included to ask whether the Ca^{2+}-binding capability of the pigment present in WT flies could influence the biochemical assays or the fluorescent images.

Cellular fractions

Membrane preparation started with 5-7 g of adult flies, and was performed according to Damiani et al. (Damiani et al., 1991), as modified by Martinez-Merlos et al. (Martinez-Merlos et al., 1997). Briefly, three fractions: total membranes (TM), low-speed pellet (LSP), and soluble fraction (SF) were obtained. Flies were homogenized with a Politron in 10 volumes of 10 mM HEPES, pH 7.4, 20 mM KCl, 0.5% CHAPS, 1 mM EGTA and one pill of the peptidase-inhibitors Complete Inhibitors (Roche, Basel, Switzerland). LSP was obtained after centrifugation of the homogenate at 650 ***g*** for 10 minutes and resuspension in 10 mM HEPES, pH 7.4, 0.5 M NaCl. The supernatants were then centrifuged at 120,000 ***g*** for 90 minutes, to obtain the SF (supernatant) and the TM (pellet) fractions. TM, including mitochondrial and microsomal membranes, was resuspended in 0.3 M sucrose, 10 mM imidazole, pH 7.4 with the peptidases-inhibitor Complete Inhibitors. This method allows suitable membrane preparations for [^{3}H]-ryanodine and [^{3}H]-IP_3 binding using small portions of tissue (Damiani et al., 1991).

The protocol for the microsomal fraction was similar to the one mentioned above, except for the centrifugation cycles (Aguilar-Delfín et al., 1996): (1) 1000 ***g*** for 10 minutes; (2) supernatant then centrifuged at 9500 ***g*** for 30 minutes; (3) second supernatant ultracentrifuged at 110,000 ***g*** for 90 minutes; and finally (4) the pellet containing the crude microsomal fraction was resuspended and stored as above. Protein concentration was quantified following Lowry et al. (Lowry et al., 1951) with bovine serum albumin as standard.

[^{3}H]-ryanodine and [^{3}H]-IP_3-binding assays

[^{3}H]-ryanodine was incubated for 16 hours at room temperature with 100 μg of the *Drosophila* TM or the microsomal fraction in 0.25 ml of binding buffer containing 200 mM MOPS, pH 7.4, 1 mM $CaCl_2$, 0.3 M KCl, 10 mg/ml bovine serum albumin (BSA) and 3 nM [^{3}H]-ryanodine (Chu et al., 1990). Non-specific binding was defined using 10 μM unlabeled ryanodine. At the end of the incubation time, the samples were filtered through Whatman GF/F glass fiber filters using a multifilter harvester (Brandel, Gaithersburg, MD). The filters were washed with five 5 ml aliquots of cold 0.3 M KCl and counted in a liquid scintillation counter, after the addition of 5 ml of Tritosol (Fricke, 1975). Free Ca^{2+} concentrations in the samples were calculated with the program Chelator (Schoenmakers et al., 1992).

[^{3}H]-IP_3 was incubated for 30 minutes at 0°C with 100 μg of *Drosophila* TM or microsomal fraction in 120 μl of binding buffer containing 25 mM Tris-HCl, pH 8.5, 5 mM $NaHCO_3$, 1 mM EDTA, 0.25 mM DTT and 4 nM [^{3}H]-IP_3 following Furiuchi et al. (Furiuchi et al., 1993). Non-specific binding was defined with 10 μM of unlabeled IP_3. The samples were filtered through Whatman GF/F glass fiber filters using a multifilter harvester (Brandel, Gaithersburg, MD). The filters were then washed with five 5 ml aliquots of a buffer containing 25 mM Tris-HCl, pH 8.0, 5 mM $NaHCO_3$ and 1 mM EDTA, and counted in a liquid scintillation counter, after the addition of 5 ml of Tritosol (Fricke, 1975). In both assays, Scatchard plots were analyzed by linear regression.

Measurement of Ca^{2+} and Mg^{2+} ATPases activities

ATPase activities were measured following Saborido et al. (Saborido et al., 1999), by using the coupled enzymatic assay of Chu et al. (Chu et al., 1988), where the rate of ATP hydrolysis is calculated from the spectrophotometric data of NADH oxidation at 340 nm.

To measure the combined Ca^{2+} and Mg^{2+} ATPases activities, the reaction mixture (1 ml final volume) contained 1 μg of protein of microsomal membranes, 19.5 mM MOPS, pH 7.0, 0.78 mM EGTA, 11.7 mM $MgCl_2$, 156 mM KCl, 10 mM phosphoenol pyruvate, 4 μM of the Ca^{2+} ionophore A23187, 9.1 units of pyruvate kinase, 5.7 units of lactate dehydrogenase, 0.3 mM NADH and 0.78 mM $CaCl_2$. To eliminate the contribution of the Ca^{2+} ATPase to the reaction, 16.4 mM $CaCl_2$ was added to the reaction mixture in parallel assays. The assays started with the addition of 4 mM ATP and the ATPases activities were followed by a decrease in optical density at 340 nm for the next 3-5 minutes. Additionally, we repeated this assay including two ionophores (nigericin 1 μm and valinomycine 10 μm) besides the calcium ionophore A23187, to control for possible iontophoretic effects of thapsigargin at the concentrations used. Results were not significantly different from assays without the ionophores (n=5).

The sensitivity of the Ca^{2+} ATPase to thapsigargin was measured in the same conditions described above, but in the presence of 20, 50, 80, 100, 120 and 150 μM of thapsigargin (Calbiochem, San Diego, CA).

Confocal microscopy

Embryos

Adults were allowed to lay eggs on fruit juice agar plates seeded with yeast paste at 25°C for 3 hours. The embryos were collected with a paintbrush onto a mesh, rinsed with distilled water, and dechorinated in 50% chlorox, rinsed with water, and transferred to microfuge tubes. Next, they were permeabilized in heptane for 30 seconds, followed by the addition of fixing solution (37% formaldehyde in phosphate buffered saline solution (PBS) and 50 mM EGTA, pH 7.5) and incubated with gentle agitation for 1 minute. The viteline membrane was removed by shaking the embryos vigorously for 1 minute after adding 1 ml of 100% methanol to the tubes and having removed the fixing solution. Finally, embryos were rehydrated in PBS and incubated with 1 μM BODIPY TR-X Ryanodine, or 5 μM BODIPY FL-Thapsigargin, or 2 μM FL-Heparin (Molecular Probes, Eugene, Oregon), or combinations of the above for 2 hours. To perform the

experiments with FL-Heparin, it was necessary to treat the embryos with 0.3% Triton-X 100 for 2 hours before the addition of the fluorescent compound. To estimate non-specific binding, control embryos were incubated with 100 μM ryanodine, thapsigargin, and heparin, and the correspondent fluorescent derivative, respectively. After incubation, embryos were washed twice with PBS, placed on microscope slides and observed on a NIKON PCM2000 confocal microscope (Cifuentes et al., 2001).

Adults

Organisms under CO_2 anesthesia were immersed on Tissue-Tek and frozen (Leica, Nussloch, Germany). 8-μm-thick cryostat sections were cut (Leica, Nussloch, Germany), dried for 30 minutes at 60°C, fixed in 3% glutaraldehide for 30 minutes at 37°C, and incubated with the fluorescent compounds using the same conditions as embryos (Thompson et al., 1997). Controls for non-specific binding were done as mentioned above.

Database searches

Complete amino acid sequences corresponding to 15 RyRs (10 species), 13 IP_3Rs (8 species), and 21 SERCAs (14 species) were obtained from the Swiss-Prot and NCBI sequence banks. *Drosophila*, other invertebrate, and different vertebrate isoforms were used for sequence examination and construction of phylogenetic trees. On average, the number of total amino acids corresponding to each protein was: RyR, 5200; IP_3Rs, 3250; SERCAs, 300. Proteins and species used in the study are listed in Table 1.

Multiple-sequence alignment and phylogeny

Full-length proteins were initially aligned using the program CLUSTALX, version 1.8.1 (Thompson et al., 1997). We employed the Program BLAST-2 SEQ 2.2.2 to assess sequence relatedness using the whole set of amino acids of each protein and a PAM distance (number of accepted point mutations per 100 residues separating two sequences) below 250 (Tatusova and Madden, 1999). Using PHYLO_WIN (Galtier et al., 1996), phylogenetic trees were constructed by maximum parsimony and distance methods. A distance matrix of pairwise comparisons of the proportion of different amino acids per site was constructed using PROTDIST of PHYLIP, version 3.572c (Hillis, 1991). This program was used to derive a neighbor-joining tree whereas maximum-parsimony analysis was done using PHYLIP-PROTPARS (Hillis, 1991). To assess support at each node, Bootstrap resampling analysis was performed (Galtier et al., 1996). However, only a limited number of replicates were done with Bootstrap analysis, since the capacity of the program was reached due to the large size of the protein sequences studied. The hierarchical structure of the trees was confirmed by the g1 statistic test (Felsenstein, 1996). Phylogenetic trees were displayed with the program TREEVIEW 1.6.6 (Page, 1996).

Results

[^{3}H]-ryanodine-binding assays

Fig. 1A shows a saturation curve with increasing concentrations of [^{3}H]-ryanodine in TM fractions of adult *Drosophila*. The saturation curve was hyperbolic but linear with Scatchard

Table 1. Identity between the amino acid sequence of RyR, SERCA and IP_3R of *Drosophila* and other invertebrate and vertebrate species

Ryanodine receptor		Ca^{2+} ATPase		IP_3 receptor	
Invertebrates	Identity (%)	Invertebrates	Identity (%)	Invertebrates	Identity (%)
Drosophila melanogaster	100	*Drosophila melanogaster*	100	*Drosophila melanogaster*	100
Caernohabditis elegans	45	*Schistosoma mansoni*	73	*Caernohabditis elegans*	36
		Patinopecten yessoensis	75	*Panulirus argus*	57
		Procambarus clarkii	81		
Type 1					
Makaira nigricans	41	*Makaira nigricans*	71	*Mus musculus*	56
Rana catesbaiana	43	*Oryctolagus cuniculus*	71	*Rattus norvergicus*	56
Sus scrofa	43	*Rana esculenta*	73	*Bos taurus*	56
Oryctolagus cuniculus	43	*Rattus norvergicus*	72	*Xenopus laevis*	56
Homo sapiens	43	*Gallus gallus*	73		
		Homo sapiens	71		
Type 2					
Oryctolagus cuniculus	44	*Sus scrofa*	72	*Rattus norvergicus*	53
Mus musculus	44	*Rattus norvergicus*	72	*Homo sapiens*	53
Homo sapiens	37	*Mus musculus*	72	*Bos taurus*	53
		Gallus gallus	72		
		Felis silvestris catus	72		
		Canis familiaris	72		
		Homo sapiens	72		
Type 3					
Rana catesbaiana	43	*Rattus norvergicus*	67	*Rattus norvergicus*	50
Oryctolagus cuniculus	43	*Mus musculus*	68	*Bos taurus*	50
Gallus gallus	40	*Gallus gallus*	69	*Homo sapiens*	50
Mustela vison	40	*Homo sapiens*	67		

Full length proteins were aligned with the program CLUSTALX 1.8.1. Relatedness between *Drosophila* protein sequences and the protein sequences of other species was obtained with the program BLAST-2 SEQ. The number of accepted point mutations per 100 residues separating two sequences (PAM) was below 250.

Drosophila melanogaster, fruit fly; *Caenorhabditis elegans*, nematode; *Makaira nigricans*, marlin fish; *Rana catesbaiana*, bull frog; *Sus scrofa*, pig; *Oryctolagus cuniculus*, New Zealand rabbit; *Homo sapiens*, humans; *Mus musculus*, house mouse; *Gallus gallus*, chicken; *Mustela vison*, american mink; *Panalirus argus*, american lobster; *Rattus norvegicus*, Wistar rat; *Bos taurus*, cow; *Xenopus leavis*, African frog; *Schistosoma mansoni*, Manson's blood fluke; *Patinopecten yessoensis*, yesso scallop; *Procamburus clarkii*, red swamp crayfish; *Canis familiaris*, dog; *Rana esculenta*, edible frog; *Felis silvestris catus*, cat.

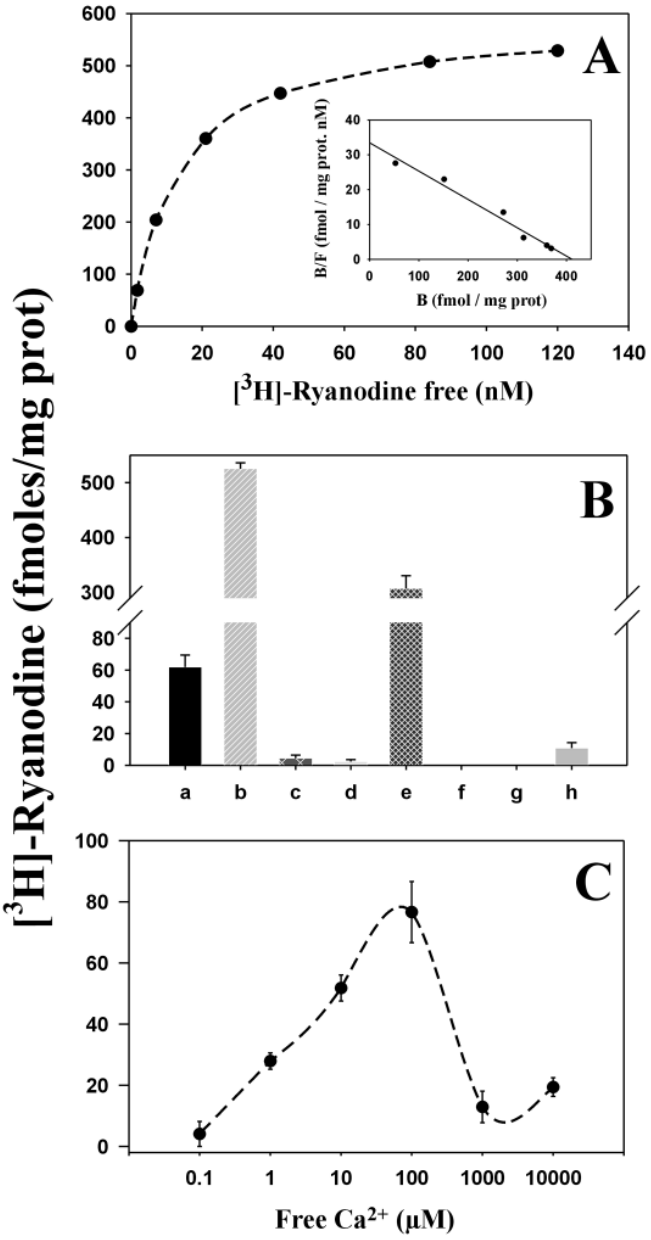

Fig. 1. Scatchard analysis, pharmacological profile and Ca^{2+}-dependence of [^{3}H]-ryanodine binding to *Drosophila melanogaster* microsomal membrane fractions. Experiments were performed with 100 μg of microsomal protein and the presence of 1-120 nM (A) or 5 nM [^{3}H]-ryanodine (B,C) as described in Materials and Methods. Panel A illustrates a hyperbolic saturation curve as a function of increasing ryanodine concentrations. The inset shows a linear Scatchard plot. This is a representative experiment from a total of 5. Panel B depicts the effects of several activators and inhibitors of RyR in comparison with control conditions (column a). column b, AMP-PCP 2 mM; column c, 10 mM $MgCl_2$; column d, 5 μM Ruthenium Red; column e, 10 μM xanthine; column f, 2 μM dantrolene; column g, 10 nM free Ca^{2+}; column h, the addition of 5 mM caffeine. Panel C represents the [^{3}H]-ryanodine binding to *Drosophila* microsomal membranes as a function of increasing Ca^{2+} concentrations. The free concentrations of the cation (100 nM to 10 mM) was adjusted using EGTA and according to the Chelator program (Tatusova and Madden, 1999). The results in B and C are expressed as mean±s.e.m. of five independent experimental observations; where not shown, errors bars are smaller than symbols.

analysis (Fig. 1A, inset). The parameters obtained were: Bmax=0.42±0.06 pmol/mg of protein, with a K_d of 8.1±1.2 nM and a Hill coefficient of 1.0±0.2 (n=5). Similar binding constants were found when Oregon and Yellow-White stocks of *Drosophila* were used as sources of subcellular fractions (data not shown). Comparable results were attained when the microsomal fraction was used (data not shown).

Fig. 1B illustrates the pharmacological profile of *Drosophila* RyR evaluated by [^{3}H]-ryanodine-binding assays (Chu et al., 1990; Antaramián et al., 2001). In agreement with results from vertebrate type 1, 2 and 3 RyRs (Antaramián et al., 2001; Zarka and Shashan-Barmatz, 1993; Manunta et al., 2000; Holmberg and Williams, 1990), AMP-PCP (1 mM) promoted a significant increment in [^{3}H]-ryanodine binding (8.6 times over control). Caffeine (10 mM) enhanced [^{3}H]-ryanodine binding in low (10 nM) free Ca^{2+}, consistent with vertebrate results (Fig. 1B). We also tested the activator xanthine in the nM range. Some of us have characterized xanthine (5-10 nM) as an excellent activator of the rabbit RyR type 1 (Butanda-Ochoa et al., 2003). Xanthine also promoted an important activation of the *Drosophila* RyR (5.3 times more than control; Fig. 1B). $MgCl_2$ (1 mM), Ruthenium Red (10 μM) and Dantrolene (50 μM) drastically inhibited (90-98%) [^{3}H]-ryanodine binding.

Fig. 1C depicts the effect of increasing free Ca^{2+} concentrations on [^{3}H]-ryanodine binding with *Drosophila* TM fractions. Like vertebrate RyRs, *Drosophila* RyR shows a gaussian profile of [^{3}H]-ryanodine binding as a function of Ca^{2+} concentration, with a maximum at approximately 100 μM. The Ca^{2+}-promoted activation presented an EC_{50} between 1 and 10 μM, whereas the IC_{50} occurred between 100 μM and 1 mM of free Ca^{2+}. [^{3}H]-ryanodine binding was always detectable in these assays, even with 10 mM free Ca^{2+}.

[^{3}H]-IP_3-binding assays

Fig. 2 shows a representative [^{3}H]-IP_3 saturation curve, the corresponding Scatchard analysis (Fig. 2A), and the effects of heparin 10 μg/ml, 2-aminoethoxydiphenyl borate (2-APB) 75 μM, and xestospongin C 5 μM on the [^{3}H]-IP_3 binding (Fig. 2B). Only one high affinity binding site was detected for [^{3}H]-IP_3 in the TM fraction. The Scatchard analysis indicated a Bmax=6.1±0.8 pmol/mg protein, a K_d of 7.3±0.9 nM and a Hill coefficient of 1.0±0.1. Similar binding constants were found when WT and YW stocks of *Drosophila* were used (data not shown). [^{3}H]-IP_3 binding to *Drosophila* TM fractions was inhibited 75% by 1 mg/ml heparin, 85% by 75 μM 2-APB, and 90% by 5 μM xestospongin C.

Mg^{2+} and Ca^{2+}-ATPases activities – thapsigargin sensitivity

We measured Mg^{2+} and Ca^{2+} ATPases activities in *Drosophila* microsomal fractions to characterize the thapsigargin-sensitive Ca^{2+} ATPase (Fig. 3). We employed the procedure reported by Saborido et al. (Saborido et al., 1999). First, so-called ‘total’ ATPase activity was determined: Mainly Mg^{2+} and Ca^{2+}-ATPase activities. Then, we determined the ‘basal’ or ‘background’ ATPase activity; that is, ATPase activity under conditions where Ca^{2+}-ATPase is inhibited. The difference between ‘total’ and ‘basal’ is SERCA activity. Fig. 3A shows that both WT and YW stocks of *Drosophila* presented similar

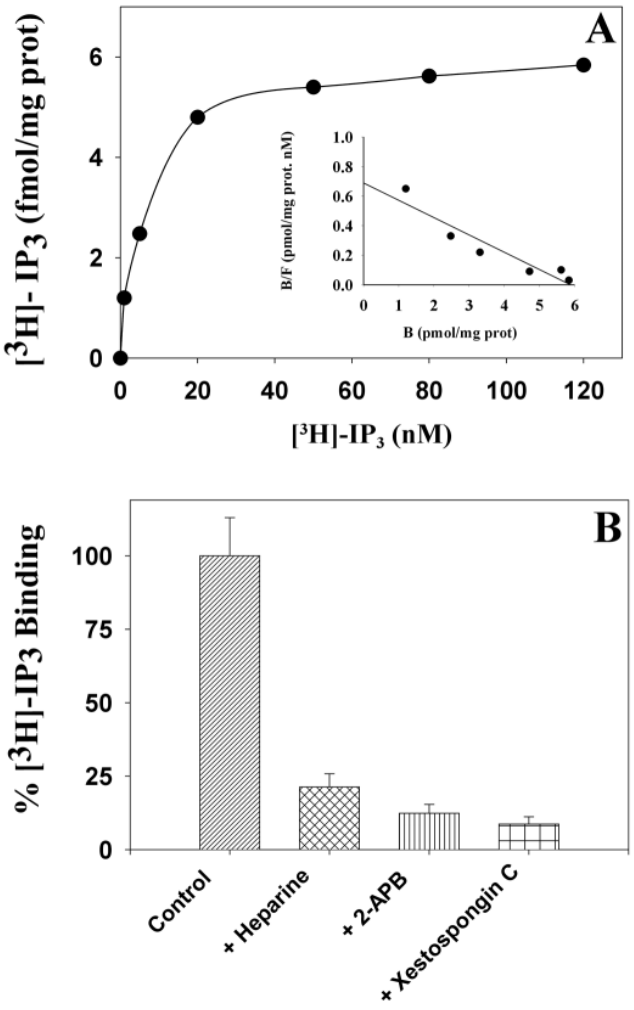

Fig. 2. Scatchard analysis and pharmacological profile of [^{3}H]-IP$_3$ binding to *Drosophila melanogaster* microsomal membrane fractions. Experiments were performed with 100 μg of microsomal protein and the presence of 1-120 nM (A) or 3 nM [^{3}H]-IP$_3$ (B) as described in Materials and Methods. Panel A illustrates a hyperbolic saturation curve as a function of increasing IP$_3$ concentrations. The inset shows a linear Scatchard plot. This is a representative experiment from a total of 5. Panel B depicts the inhibitory effect of 1 mg/ml heparin, 75 μM 2-APB and 5 μM xestospongin C on [^{3}H]-IP$_3$ binding. The results in Panel B are expressed as mean±s.e.m. of at least four independent experimental observations.

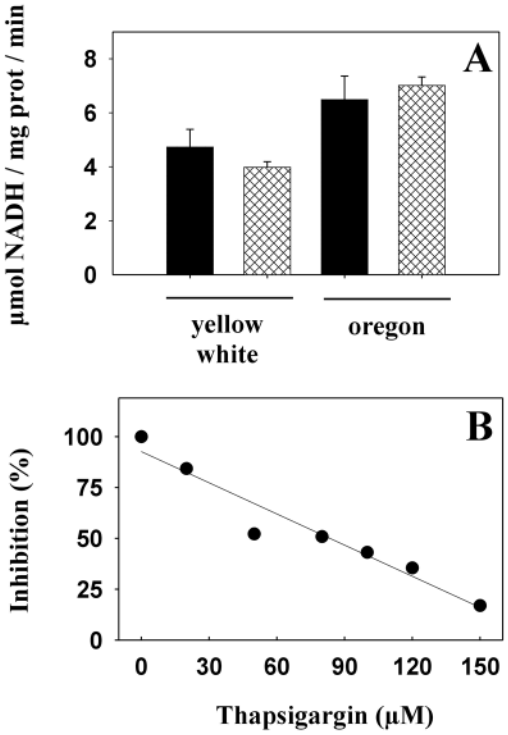

Fig. 3. Ca^{2+} and Mg^{2+}-ATPase activities in *Drosophila melanogaster* microsomal membrane fractions: thapsigargin sensitivity. Experiments were done with 1 μg of microsomal protein as outlined in Materials and Methods. Panel A indicates the activities of Mg^{2+} (filled) and Ca^{2+}-ATPases (crosshatched). Different ATPases activities were obtained in the WT and YW stocks used. The results are expressed as mean±s.e.m. of five independent experimental observations. Panel B shows the inhibition of the Ca^{2+}-ATPase activity promoted by increasing concentrations of thapsigargin. The results are the mean of 5 independent experimental observations. Standard errors are not shown, but in all cases were smaller to 15% of the mean value. The IC_{50} obtained for thapsigargin was 80 μM.

total activities. However, WT activities were ≈70% of YW, with ≈4 μmols NADH/mg protein/minute in WT, and ≈6.2 μmols NADH/mg protein/minute in YW.

Drosophila SERCA was sensitive to thapsigargin (Fig. 3B). This is shown by inhibition of SERCA activity in both WT and YW microsomal membranes in the presence of different amounts of thapsigargin. The IC_{50} for this sesquiterpene lactone was approximately 80 μM. In this assay, Ca^{2+}-ATPase activity was also inhibited by the addition of EGTA (1 mM) or by high Ca^{2+} concentrations (≈20 mM) (data not shown).

Confocal microscopy studies

To characterize RyR, IP$_3$R and SERCA protein distribution in fly tissues, we used fluorescent compounds specific for RyR (TX-R-BODIPY-ryanodine), IP$_3$R (FL-Heparin), and thapsigargin-sensitive SERCA (FL-BODIPY-thapsigargin) (Figs 4, 5). Fig. 4A shows the signal associated with fluorescent ryanodine present in practically all cells of early embryos. Fig. 4D shows the label localized mainly to the cytoplasm of cells. The fluorescent ryanodine signal observed in older embryos (stages 15-17) clearly shows RyR at higher concentrations in the digestive tract (Fig. 4A'). The label associated with *Drosophila* SERCA (Fig. 4C) and IP$_3$R (Fig. 4B) in early embryos is also present in practically all cells. In late embryos [Fig. 4C' (SERCA); B' (IP$_3$R)], label is present in nearly all tissues and is distributed more homogeneously than ryanodine signals. Labeling for all three fluorescent compounds is seen in tissues derived from all germinal layers: ectoderm (epidermis), mesoderm (muscle), and endoderm (digestive tract). As seen for the ryanodine receptor, higher magnification views of cells labelled with thapsigargin and heparin also show cytoplasmic staining (Fig. 4F,E, respectively) Co-localization of these compounds with fluorescent ryanodine illustrates that SERCA and RyR are highly coexpressed in the digestive tract (Fig. 4H), whereas

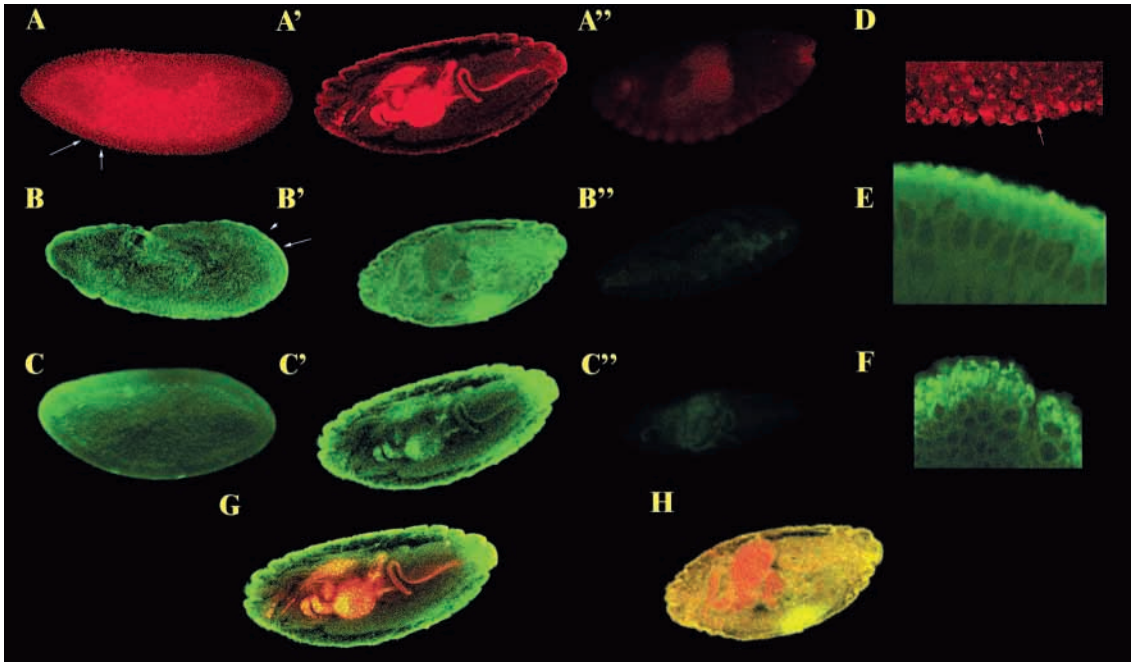

Fig. 4. Protein localization of the ryanodine receptor, IP_3 receptor and thapsigargin-sensitive Ca^{2+}-ATPase in *Drosophila melanogaster* embryos. Embryos were processed as mentioned in Materials and Methods, and then incubated with TX-R-BODIPY-ryanodine (1 μM), FL-Heparin (2 μM) and FL-BODIPY-thapsigargin (5 μM). Panels A, B and C show the profuse signal elicited by TX-R-BODIPY-ryanodine (stage 5 embryo), FL-Heparin (stage 8 embryo), and FL-BODIPY-thapsigargin (stage 5 embryo), respectively. *Drosophila* embryos are approximately 500 μm long. In all embryo panels, anterior is left, and dorsal is top. Panels A', B' and C' show the signal elicited in late embryos (stages 15-17) incubated with TX-R-BODIPY-ryanodine (1 μM), FL-Heparin (2 μM) and FL-BODIPY-thapsigargin (5 μM), respectively. To demonstrate the specificity of the fluorescent ligands, panels A'', B'' and C'' depict similar embryos but with a very decreased signal as a consequence of a pretreatment with high concentrations of ryanodine (80 μM), heparin (100 μM), and thapsigargin (120 μM), respectively. Panel D shows a 10× magnification of the area marked between the two white arrows in A, where it is possible to see the cytoplasmic localization of the signal (red arrow). Panel E illustrates a 20× magnification of the area marked between the white arrows in B, where the cytoplasmic nature of the labeling of heparin (2 μM) is clearly seen. Panel F shows a 1000× magnification of cells of an early embryo (stage 6) where the cytoplasmic labeling of FL-BODIPY-thapsigargin (5 μM) is seen. Panel G shows dual labeling of TX-R-BODIPY-ryanodine with FL-Heparin of the embryo shown in A' and C', and panel H shows dual labeling of TX-R-BODIPY-ryanodine with FL-BODIPY-thapsigargin of the embryo shown in B'. In these last two panels colocalization of signals is shown as yellow. These images are representative examples of more than 20 independent experiments.

coexpression of IP_3R and RyR is evenly distributed (Fig. 4G). Label observed in these experiments is specific, since coincubation with excess ryanodine, heparin or thapsigargin abolished labeling (Fig. 4A'' for ryanodine, Fig. 4B'' for heparin, and Fig. 4C'' for thapsigargin).

Adult tissues were stained with BODIPY TR-X Ryanodine, BODIPY FL-Thapsigargin and FL-Heparin. A generalized RyR expression was observed, with higher levels in the digestive tract (Fig. 5A,E), muscle (Fig. 5A,D,D'), and adult optic lobe and retina (Fig. A,C). Label is cytoplasmic (Fig. 5D,D',E), as in embryos. Staining is seen in tissues of ectodermal origin (nervous system, Fig. 5A,C), mesodermal origin (indirect flight and leg muscles, Fig. 5A,D,D'), and endodermal origin (digestive tract, Fig. 5A,E). Staining for heparin was seen also in practically all adult tissues (Fig. 5B), and more homogeneous in levels than RyR. Most tissues show extensive colocalization of both labels (compare Fig. 5A and B). Colocalization of fluorescent ryanodine with fluorescent thapsigargin was coincidental (Fig. 5C).

Sequence analysis and phylogenetic classification

We performed sequence analysis of RyR, IP_3R and SERCA as another way to address similarities to and differences from their vertebrate counterparts and within themselves. Computer-generated alignments of 15 RyRs, 13 IP_3Rs and 21 SERCAs were analyzed. Table 1 shows the percentage identities between the *Drosophila* RyR, IP_3R and SERCA compared with corresponding proteins from other species. The extent of identity between *Drosophila* RyR and other RyRs considered in this study was the lowest and ranged from 37% (with *Homo sapiens* RyR type 1) to 45% (with *Caenorhabditis elegans* unique RyR isoform). It was thus not possible by this means to recognize an accentuated identity among *Drosophila* RyR and any of the three vertebrate isoforms in Table 1.

The identity detected between *Drosophila* IP_3R and other IP_3Rs was intermediate and ranged from 36% (with *Caenorhabditis elegans* unique IP_3R isoform) to 57% (with *Panulirus argus* unique IP_3R isoform). In contrast with RyR isoforms, vertebrate IP_3R type 1 isoform showed a slightly higher percentage of identity with the fruit fly receptor (56%), than IP_3R type 2 (53%) and type 3 (50%). SERCA enzymes had the highest percentage of identity within themselves. The range went from 67% (with both *Rattus norvergicus* and *Homo sapiens* SERCA type 3) to 81% (with the *Procambarus clarkii* unique SERCA isoform). *Drosophila* SERCA had a slightly

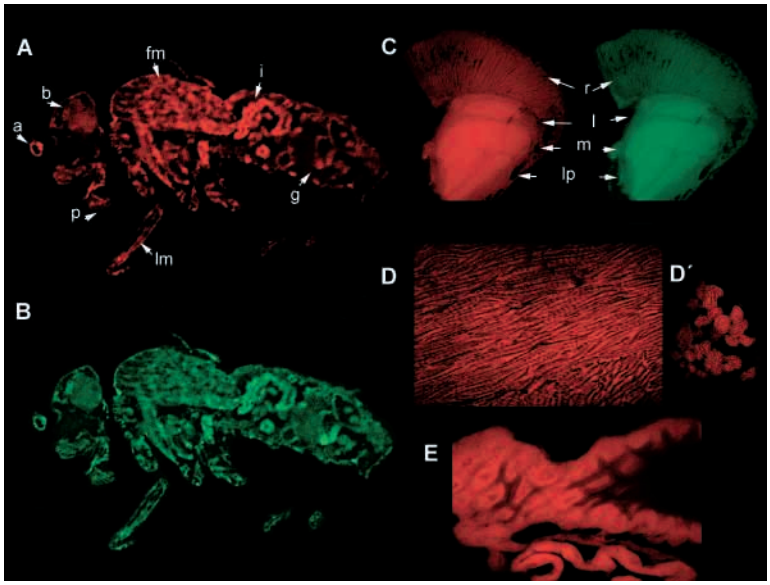

Fig. 5. Protein localization of ryanodine receptor, IP_3 receptor and thapsigargin-sensitive Ca^{2+}-ATPase in *Drosophila melanogaster* adults. Cryostat sections were processed as mentioned in Materials and Methods, and then incubated with TX-R-BODIPY-ryanodine (1 μM), FL-Heparin (2 μM) and FL-BODIPY-thapsigargin (5 μM). Panel A shows a sagital section of an adult male fly incubated with TX-R-BODIPY-ryanodine. Staining is seen in many tissues derived from all three germinal layers. Panel B is the same section as in A, but showing the signal elicited with FL-Heparin staining; profuse labeling is also seen, as in A. In both panels, intense labeling is seen in muscle (marked fm and lm in A) and in the intestine (marked i in A). Adult male flies are approximately 2-3 mm long. Panel C shows two images from the same section at 100× magnification. The image on the left shows labeling of TX-R-BODIPY-ryanodine (red) and the image on the right shows FL-BODIPY-thapsigargin (green) staining of a horizontal section of the retina and optic lobe. Intense colocalization of staining is seen in the neuropils of the optic lobe [lamina (l), medulla (m), lobula and lobula plate (lp)], with lesser staining in the photoreceptor cells and optic lobe neuronal cell bodies. As shown here, colocalization of TX-R-BODIPY-ryanodine and FL-BODIPY-thapsigargin was also coincidental in all adult tissues examined. Panel D shows a 1000× magnification of indirect flight muscles stained with TX-R-BODIPY-ryanodine in longitudinal section, where the striated pattern of labeling is evident, and panel D' shows a cross-section of leg muscles also stained with TX-R-BODIPY-ryanodine. In both cases, staining is cytoplasmic. Panel E shows a 1000× magnification of intestinal cells of an adult marked with TX-R-BODIPY-ryanodine in their cytoplasm. These sections are representative of 20 independent experiments. Abbreviations: a, antenna; b, brain; fm, indirect flight muscles; g, gonad; i, intestine; l, lamina; lm, leg muscle; lp, lobula and lobula plate (in the section in C the lobula plate is directly underneath the lobula); m, medulla; p, proboscis; r, retina and photoreceptor cells.

higher identity with vertebrate type 1 and 2 SERCAs (71-73%) than with type 3 (67-69%).

Equal-weight ('unrooted') Parsimony and Neighbor Joining analyses of the sequences were performed for RyRs, IP_3Rs (Fig. 6) and SERCAs (Fig. 7). Both programs yielded virtually identical topologies suggesting, as expected, that the three *Drosophila* proteins grouped together with all other invertebrate genes. Fig. 6A shows a phylogram where full-sequences of RyRs and IP_3Rs were analyzed together. Both types of calcium release channels were separated in the tree very clearly. *Drosophila* RyR was sister to *C. elegans* RyR, and both were in a different node from vertebrate RyRs. Type 2 and 3 RyRs were co-segregated in one group and separated from type 1 RyRs.

Drosophila IP_3R was sister to crustacean *P. argus* IP_3R, whereas the receptor of *C. elegans* split from all other IP_3Rs. Vertebrate type 1 and 2 IP_3Rs shared a common node. Fig. 5B shows the unrooted cladogram following Bootstrap analysis to determine support at each node. Topology is very similar using the PROTDIST algorithm (Fig. 6A). The cladogram shows vertebrate and invertebrate RyRs and IP_3Rs forming distinct clades within each type of calcium release channel.

Fig. 7A shows a phylogram and a cladogram (Fig. 7B) based on the analysis of amino acid sequences of SERCAs considered in this study. *Drosophila* SERCA grouped with other invertebrates and was closer to vertebrate type 1 SERCAs. Vertebrate type 3 SERCAs were the more distal proteins compared with invertebrate SERCAs (Fig. 7A,B).

Discussion

Intracellular calcium dynamics is governed mainly by the evolutionarily conserved Ca^{2+}-mobilizing elements RyR, IP_3R and SERCA. Insights into the mechanisms of intracellular calcium signaling using *Drosophila* is facilitated by virtue of the existence of single RyR, IP_3R and SERCA molecules in this model. In addition, *Drosophila melanogaster* presents a unique possibility of studying cellular signaling by multidisciplinary approaches with well established molecular, genetic, cellular, physiological, and biochemical tools. This allows better opportunities of identification and characterization of essential properties and physiological significance of these proteins in cellular extracts. Once these basic parameters are defined, the relationship of the RyR, IP_3R and SERCA from *Drosophila* with their vertebrate counterparts can be worked out. The data obtained in this study lead in this direction.

Biochemical properties of Drosophila RyR, IP_3R and SERCA

Functional studies of the *Drosophila* intracellular calcium regulation proteins are scarce. The published information does not include studies done with native membranes. For example, a report indicating the biochemical characteristics of the *Drosophila* IP_3R used S2 cells, a cellular line derived from late embryonic states (Swatton et al., 2001).

The [^{3}H]-ryanodine-binding assay is a specific, conformationally sensitive probe for the RyRs of skeletal and cardiac muscles (Takeshima et al., 1994; Pessah et al., 1987). Using this assay, we estimated the Bmax, K_d and activation state of this calcium release channel. [^{3}H]-ryanodine bound a single class of sites in the *Drosophila* microsomal preparation. The Bmax obtained for *Drosophila* RyR (0.42±0.06 pmol/mg

of protein) is lower than the value reported for rabbit sarcoplasmic reticulum heavy fraction, but is in the range of values reported for total membrane fractions of skeletal and cardiac muscles of several species of rodents (Martinez-Merlos et al., 1997). In general, the number of [^{3}H]-ryanodine-binding sites in *Drosophila* microsomal membranes is higher than the Bmax described for cerebral fractions obtained with different membrane preparations (Martinez-Merlos et al., 1997; McPherson and Campbell, 1990). The affinity of [^{3}H]-ryanodine for *Drosophila* RyR (8.1 nM) is in the range reported for almost all known vertebrate and invertebrates RyRs (Martinez-Merlos et al., 1997; Pozzan et al., 1994).

In general, the pharmacological profile of [^{3}H]-ryanodine-binding assays was similar to previously reported results for vertebrate RyRs (Chu et al., 1990; Antaramián et al., 2001). Type 1 and 3 RyRs are more prone to respond to AMP-PCP than type 2 RyRs (Antaramián et al., 2001; Zarka and Shashan-Barmatz, 1993; Manunta et al., 2000; Holmberg and Williams, 1990). Thus, the large *Drosophila* RyR activation promoted by 1 mM AMP-PCP (Fig. 3B) is closer to responses elicited by type 1 and 3 RyRs. Xanthine (at the μM range) is an oxidized purine that is a good activator of the type 1 RyR from rabbit skeletal muscle (Butanda-Ochoa et al., 2003). [^{3}H]-ryanodine binding in *Drosophila* RyR was enhanced 4-5 times by xanthine (Fig. 3B). This result is similar for both the *Drosophila* RyR and the rabbit type 1 RyR. [^{3}H]-ryanodine binding to *Drosophila* RyR was inhibited by Mg^{2+} (2 mM) and ruthenium red (10 μM), in the same way as vertebrate RyR isoforms. However, inhibition by dantrolene (Fig. 3B) makes the *Drosophila* RyR more similar to type 1 and 3 RyRs, since Zhao et al. (Zhao et al., 2001) reported that RyR type 2 is not a target for dantrolene inhibition.

The calcium sensitivity of the [^{3}H]-ryanodine-binding assay is one of the most important factors discriminating among different RyR isoforms. Whereas the type 1 and 3 RyRs show an unambiguous bell-shaped calcium dependence curve with increased sensitivity at low calcium concentrations for the RyR type 1 (Murayama et al., 1999), the RyR type 2 is not sensitive to inactivation by high calcium concentrations up to pCa 2 (Du et al., 1998). The result obtained with the calcium dependence curve of *Drosophila* RyR (Fig. 3C), indicates a pronounced similarity with RyR type 1, since the [^{3}H]-ryanodine binding was visibly present at 1 μM of free Ca^{2+} in the assay, a condition where the activity of type 3 RyRs is not observed (Murayama et al., 1999). A distinctive characteristic of *Drosophila* RyR was its capacity to bind [^{3}H]-ryanodine even at Ca^{2+} concentrations in the millimolar range (Fig. 3C). This ability is in some way similar to the low Ca^{2+} dependence of inactivation of RyR type 2. Thus, *Drosophila* RyR shares features of both RyR type 1 and 2, but is closer to RyR type 1.

Drosophila RyR, as well as vertebrate RyR isoforms, are activated by 3-methyl xanthine and caffeine (2 mM). Zhang et

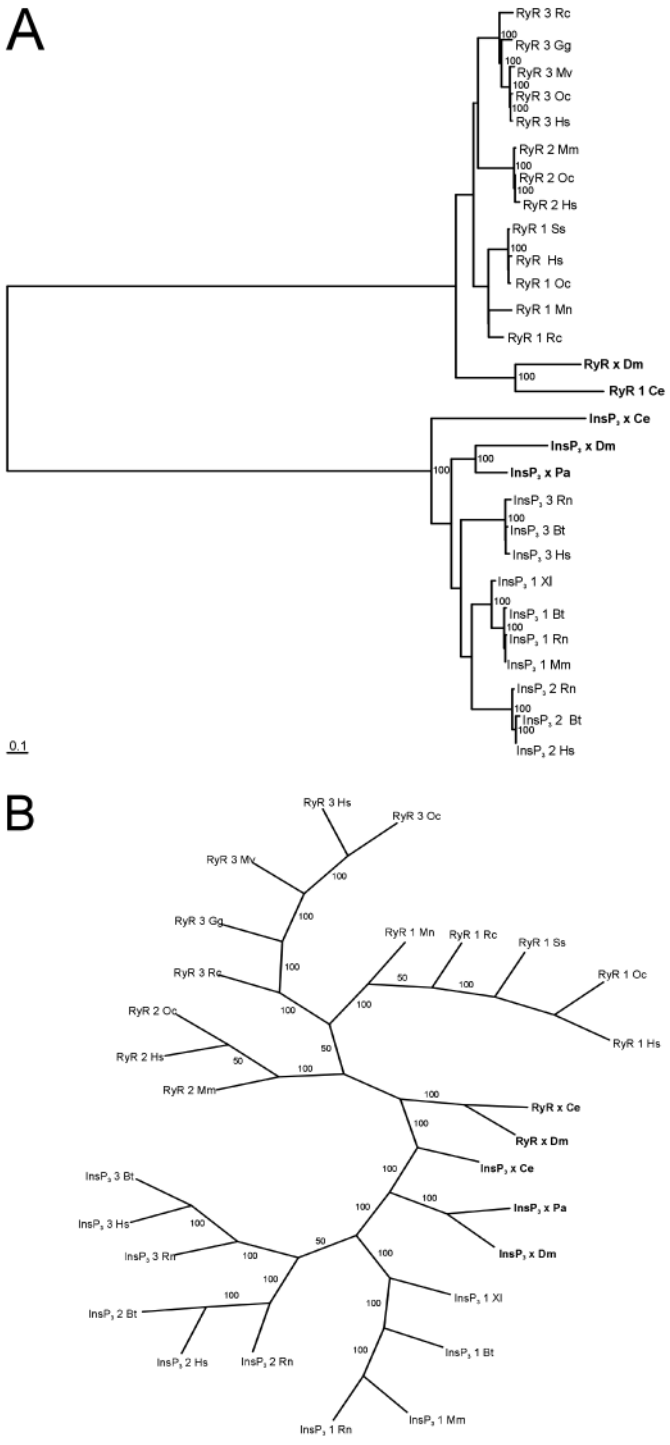

Fig. 6. Phylogenetic analyses of relationships based on comparisons of complete amino acid sequences representing 28 different RyRs and IP_3Rs. The analyses include the RyR and IP_3R from *Drosophila melanogaster*, the calcium release channels from other invertebrates as well as the three different vertebrate isoforms of these proteins from representative species. (A) Phylogram of the most parsimonius unrooted PHYLO_WIN tree recovered (1101 steps), where horizontal branch lengths are proportional to the amount of divergence along a lineage. The topology of this tree was identical to the Neighbor Joining tree (data not shown). In Panels A and B, RyR and IP_3R are depicted as 'RyR' and 'InsP3' followed by the type number (for vertebrate sequences) and the abbreviation of the species, respectively. (B) Unrooted cladogram illustrating the pattern of relationships. This tree was recovered following Bootstrap analysis (2 replicates). The number of each node indicates the percentage recovery for the node during resampling. Species code: *Drosophila*, Dm; *C. elegans*, Ce; blue marlin, Mn; pig, Ss; rabbit, Oc; human, Hs; mouse, Mm; bull frog, Rc; chicken, Gg; american mink, Mv; lobster, Pa; Wistar rat, Rn; cow, Bt; Xenopus, Xl.

al. (Zhang et al., 1999), reported that caffeine activation of lobster RyR is insensitive to Ca^{2+} concentrations, which is different from caffeine activation of vertebrate RyRs. Further experiments are needed to confirm whether this caffeine-binding site reported for lobster skeletal RyR is also present in *Drosophila* RyR.

In binding experiments using [^{3}H]-IP_3 in *Drosophila* microsomal membranes, the ligand was bound to a single class of sites (Hill coefficient=1.0). The Bmax value indicates that, in *Drosophila*, the IP_3R is 15 times more abundant than the RyR in microsomes, a proportion that is similar to that reported for cerebral tissue in several species (McPherson and Campbell, 1990; Diaz-Muñoz et al., 1999). The affinity for [^{3}H]-IP_3 found in *Drosophila* microsomal membranes (7.3 nM) was similar to the K_d reported for S2 cells (Swatton et al., 2001) and for the mammalian IP_3Rs subtypes including type 1 from rat cerebellum and type 2 from rat liver (Correa et al., 2001).

[^{3}H]-IP_3 binding to microsomal membranes of *Drosophila* was inhibited by the competitive antagonist heparin (Fig. 2B) to a similar extent to that of vertebrate IP_3Rs (Mikoshiba et al., 1994). Unexpectedly, the noncompetitive IP_3R inhibitors, 2-APB and xestospongin C, reduced notably the [^{3}H]-IP_3 binding to *Drosophila* microsomal membranes. These results are in contrast with reports showing that 2-APB and xestospongin C abolished ion transport through IP_3R without affecting the ability of [^{3}H]-IP_3 to bind to microsomes from CHO cells and cerebellum, respectively (Kukkonen et al., 2001; Gafni et al., 1997). Further experiments exploring the inhibitory mechanism(s) of these drugs are needed to clarify the discrepancy between the pharmacological properties of *Drosophila* and vertebrate IP_3Rs.

Another difference in the pharmacological profile between *Drosophila* IP_3R and its vertebrate counterparts, is its increased sensitivity to the agonist adenophostin A (Swatton et al., 2001). This means that the recognition site for adenophostin could have different properties in the *Drosophila* IP_3R.

Given the high homology (≈70%) between *Drosophila* SERCA and the rest of the SERCA enzymes included in Table 1, it is very likely that most of the structure/function relationships and the mechanism of SERCA Ca^{2+} transport in vertebrate fast twitch skeletal muscle (MacLennan et al., 1997), are also present in this insect ATPase. The SERCA activity measured in *Drosophila* microsomal membranes was in the same range as those reported elsewhere for vertebrate isoforms (Saborido et al., 1999; Chu et al., 1988). Thapsigargin is a specific inhibitor of SERCAs, and has been used as a pharmacological probe to detect this family of enzymes. The inhibitory mechanism of this sesquiterpene lactone is to bind the enzyme during the Ca^{2+}-deprived intermediate state, being usually effective at sub-nM concentrations (Mintz and Guillan, 1997). High micromolar concentrations of thapsigargin (like the ones we used) can act as a Ca^{2+} ionophore (Favero and Abramson, 1994), but since our SERCA activity assay is done in the presence of the well known Ca^{2+} ionophore A23187, an iontophoretic activity of thapsigargin is not critical for interpretation of our results. The thapsigargin sensitivity that we observed in *Drosophila* microsomes was in the micromolar range (Fig. 3B). This clear discrepancy with previous reports, and also with the observation made in saponine-permeabilized S2 cells, could involve changes in the properties of the enzyme due to microsomal membrane preparation. Further experiments

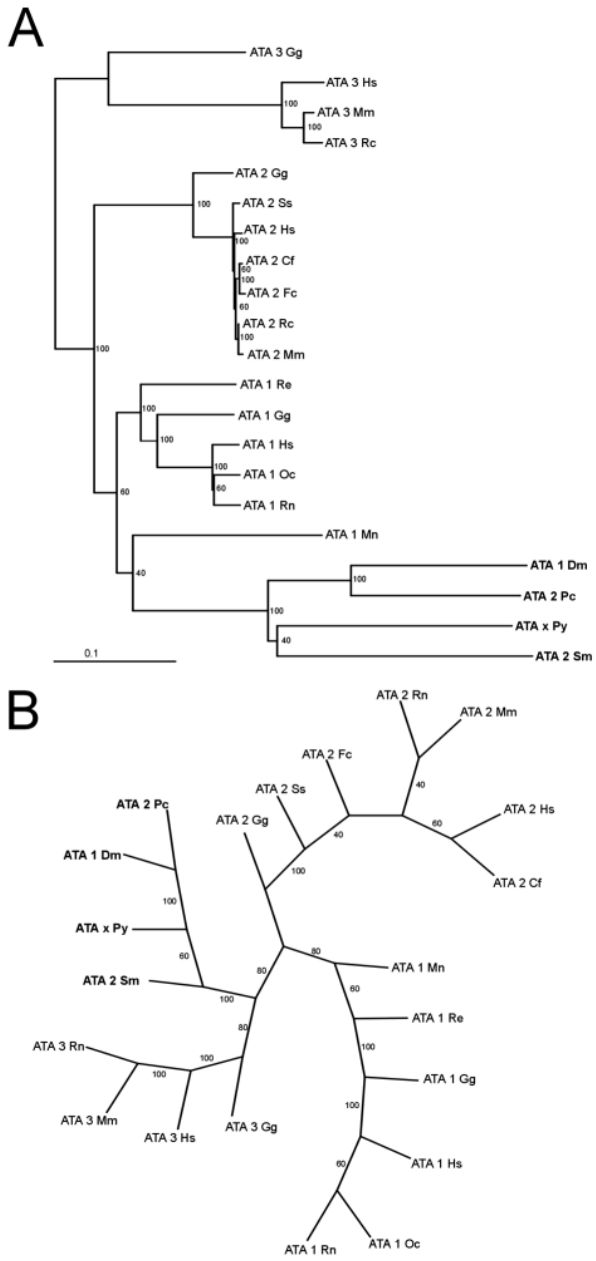

Fig. 7. Phylogenetic analyses of relationships based on comparisons of complete amino acid sequences representing 21 different sarco(endo)plasmic reticulum Ca^{2+}-ATPases (SERCAs). The analyses include the SERCA from *Drosophila melanogaster*, the SERCAs from other invertebrates as well as the three different vertebrate isoforms from representative species. (A) Phylogram of the most parsimonius unrooted PHYLO_WIN tree recovered (1369 steps), where horizontal branch lengths are proportional to the amount of divergence along a lineage. The topology of this tree was identical to the Neighbor Joining tree (data not shown). In Panels A and B SERCAs are depicted as 'ATA' followed by the type number (for vertebrate sequences) and the abbreviation of the species. (B) Unrooted cladogram illustrating the pattern of relationships. This tree was recovered following Bootstrap analysis (5 replicates). The number of each node indicates the percentage recovery for the node during resampling. Species code: *Drosophila*, Dm; blood fluke, Sm; yesso scallop, Py; crayfish, Pc; human, Hs; dog, Cf; cat, Fc; chicken, Gg; blue marlin, Mn; mouse, Mm; rabbit, Oc; edible frog, Re; Wistar rat, Rn; pig, Ss.

are also needed to clarify this point. Also, the fact that the YW stock had a higher activity than the WT stock might be related to the amount of pigment present within the cells.

The Mg^{2+}-ATPase activity measured according to Saborido et al. (Saborido et al., 1999), is designed to evaluate the activity of E-type ATPases, and so it could be that the activity we measured in the *Drosophila* microsomal fraction is of E-type. Additional experiments are necessary to characterize the sensitivity of this enzymatic activity to specific inhibitors and substrates, to compare SERCA with other E-type Mg^{2+}-ATPases (Plesner, 1995).

Drosophila RyR, IP_3R and SERCA anatomical localization

Fluorescently tagged ryanodine labeled nearly all cells in early and late embryos (Fig. 4). Label is cytoplasmic, consistent with labeling of endoplasmic reticulum (Fig. 4D). This generalized labeling is maintained throughout embryogenesis (Fig. 4A'), but some areas, like the digestive tract, accumulate higher amounts of label. Staining of adult fly cryostat sections showed similar results. Notably, the nervous system showed staining, albeit not particularly high, in agreement with behavioral and electrophysiological studies that have yet to show nervous system functional deficits in RyR and IP_3R mutants (Acharya et al., 1997) and a report showing adaptation deficits to odorant stimuli in antennal electrophysiological recordings in IP_3R receptor mutants (Deshpande et al., 2000). Results with both fluorescently tagged heparin and thapsigargin show overall similarities: early embryos show promiscuous staining in nearly all cells, and late embryos show staining in nearly all tissues with the digestive tract showing higher levels of staining. This higher level of digestive tract staining is more prominent with heparin. In both cases staining appears to be cytoplasmic, consistent with labeling of the endoplasmic reticulum (Fig. 4). Double labeling experiments show that, as expected, the digestive tract has generalized overlapping staining, with a preponderance of ryanodine staining (Fig. 4G,H).

These RyR results are in contrast with in situ hybridization experiments, where expression of RyR is seen at stage 9 at the earliest (Sullivan et al., 2000), and not as widespread as here. We interpret this as maternal contribution: ryanodine is well known as a very specific pharmacological binding agent for the RyRs (Chu et al., 1990; Pessah et al., 1987). Since we were able to outcompete the staining with non-fluorescent ryanodine, we conclude that RyR protein is present from the very early stages, with a subcellular localization consistent with its purported role in intracellular Ca^{2+} homeostasis.

The difference between our results and those obtained through in situ hybridization experiments could be due to the presence of maternally deposited RyR protein, and also, to low levels of RyR expression, levels not readily demonstrable by in situ hybridization. Our data complements mRNA expression data, and thus, offer a more comprehensive view of localization and function of RyR. It would be of interest to stain developing oocytes and females ovaries to further these results.

The localization of IP_3R also shows similar differences with respect to in situ hybridization data: published in situ data offer a very restricted expression pattern, with higher levels in late embryos in prospective antenno-maxillary complex (a complex comprising the dorsal and terminal organs) and the labial organ (Hasan and Rosbash, 1992; Raghu and Hasan, 1995) [(Campos-Ortega and Hartenstein, 1997) for sensory organ nomenclature]. In contrast, our data reveal widespread expression of the IP_3R protein; consistent with mutant defects, expression of the protein occurs at all stages and tissues. There is also high expression in the digestive tract, again consistent with the requirement for intracellular Ca^{2+} dynamics in visceral muscle function and consistent with immunocytochemistry data (Raghu and Hasan, 1995). Staining has less marked regional differences than RyR staining. Our data support the idea that IP_3R protein, like RyR protein, is also contributed maternally and/or is expressed at levels not readily detectable by in situ hybridization at all stages and tissues. This underscores the value of examining both transcript and protein expression data, although some caution should be exercised as heparin may label other proteins besides IP_3R protein.

Finally, *Drosophila* SERCA expression has not been reported before. We find widespread embryonic expression, with little or no regional differences (Fig. 4C,C'). Thapsigargin also shows widespread staining in adult tissues (Fig. 5C). There is ample colocalization of RyR and SERCA protein expression in embryonic and adult tissues, evidenced by the general overlap between RyR and SERCA (thapsigargin) staining. The embryonic digestive tract stands out in double labeling experiments because the amount of RyR is so strong that it quenches the SERCA staining present in the digestive tract (compare Fig. 4C',H). Elsewhere, levels are less disparate (Fig. 5C). This generalized co-localization is consistent with the largely complementary function of both proteins in intracellular Ca^{2+} dynamics. Overall, our data support the involvement of these proteins in intracellular Ca^{2+} dynamics and muscle function, but point to a more general role in all cells and tissues.

Molecular evolution of Drosophila RyR, IP_3R and SERCA

The homology between the *Drosophila* RyR and other RyRs, like the *C. elegans* gene and the three vertebrate ones, was in all cases around 40% (Table 1). Thus, it is not possible to deduce relationships between the invertebrate receptors and their vertebrate counterparts from sequence data. However, inspection of the phylogram and cladogram in Fig. 6 indicates that the *Drosophila* and *C. elegans* RyRs form a separate group from the vertebrate isoforms. It might seems premature to assign the *Drosophila* and *C. elegans* RyRs as type 1 based only in their conspicuous muscular localization (Takeshima et al., 1994; Maryon et al., 1996), but biochemical data support such a tenet. Taken together, evidence points to a closer relationship between vertebrate RyR type 1 and invertebrate RyR.

IP_3Rs are different: the homology between the *Drosophila* IP_3R and the IP_3R from *C. elegans* was smaller (36%) than with the vertebrate isoforms 2 (53%), 3 (50%) and 1 (56%), or the lobster IP_3R (57%) (Table 1). The data may suggest that the *Drosophila* IP_3R is closer to the vertebrate IP_3R type 1 than the other 2 isoforms. One can speculate that this state of affairs is due to evolutionary divergence since the last common ancestor between nematodes and arthropods/vertebrates

happened earlier in time than the split between arthropods and vertebrates. Once the vertebrate lineage split from the arthropods, several duplication events in the vertebrate lineage gave rise to the current three isoforms. It can be added that similarities in homology values among all RyRs considered could be explained by somewhat different structural constraints in RyRs compared to IP_3Rs.

RyRs and IP_3Rs are homologous proteins sharing 30-35% homology at the amino acid level. However, there are three regions where the homology is higher: (1) the first 600 amino acids (numbering based on RyRs sequences), (2) the central region between amino acids 1500 and 2600, and (3) the C-terminal domain starting from residue 3900, containing the transmembrane domains (Sorrentino et al., 2000). The phylogenetic tree of the intracellular calcium release channel family presented in Fig. 6 is an extension of previous studies (Takeshima et al., 1994; Franck et al., 1998). Both the phylogram and the cladogram in Fig. 6 show that the RyRs and IP_3Rs from invertebrates are grouped separately from vertebrate isoforms. Vertebrate isoforms could have diverged because they specialized to fulfill physiological requirements of determined tissues; for example, RyR type 1 allows the excitation-contraction coupling of skeletal muscle, whereas RyR type 2 does the same in cardiac muscle. What is the strategy used in invertebrates? There are three possibilities: first, that in *Drosophila* and other invertebrates the specialized roles of each receptor can be accomplished by alternatively spliced forms of the RyR and IP_3R genes; second, that the intrinsic molecular properties of each receptor enable them to carry out all the different functions encompassed by their vertebrate counterparts; or third, that owing to the different nature of tissues in vertebrates and invertebrates, such specialized roles are not required.

The Ca^{2+} ATPases of intracellular stores clearly derived from their plasma membrane counterparts early in the evolution of eukaryotes (Carafoli and Klee, 1999). Table 1 shows that, overall, SERCAs from *Drosophila* and other invertebrates present somewhat higher levels of identity with vertebrate SERCA1 and SERCA2 (71-73%), and somewhat less with SERCA type 3 (67-69%). From the phylogram and cladogram in Fig. 7 it seems that invertebrate SERCAs are perhaps closer to vertebrate type 1 SERCAs. Vertebrate type 1 SERCAs are characteristic of fast-twitch skeletal muscle in mammals (Brandl et al., 1987). Loss of its function in humans causes Brody disease, a debilitating but not lethal human disorder (Ordermatt et al., 1996). Interestingly, SERCA type 1 of *Makaira nigricans* (blue marlin) is in a different node from the rest of the other vertebrates, in a position closer to invertebrates. It may be that this pelagic fish has retained more of characteristics of the common SERCA ancestor due to its demand for high speed travel. It would be of interest to examine SERCAs from other fast swimming fish, such as Tuna, to see whether this is indeed a possibility.

We thank Fernando López-Barrera for help with figures. The assistance of Rafael Favila-Humara and Leopoldo González-Santos in the use of the PHYLO_WIN program is appreciated, and of Luis Vaca, Arturo Hernández-Cruz and Luis Oropeza for use of the confocal microscope at the Instituto de Fisiología Celular. This work was supported by CONACyT (projects 28055-N to M.D.-M., J27954-N and 36040-N to J.R.R.-E.) and DGAPA (projects IN 200500 to M.D.-M. and IN 209798 to J.R.R.-E.).

References

Acharya, J. K., Jalink, K., Hardy, R. W., Hartenstein, V. and Zuker, C. S. (1997). $InsP_3$ receptor is essential for growth and differentiation but not for vision in Drosophila. *Neuron* **18**, 881-887.

Aguilar-Delfín, I., López-Barrera, F. and Hernández-Muñoz, R. (1996) Selective enhancement of lipid peroxidation in plasma membrane in two experimental models of liver regeneration: partial hepatectomy and acute $CC1_4$ administration. *Hepatology* **24**, 657-662.

Antaramián, A., Butanda-Ochoa, A., Vázquez-Martinez, O., Diaz-Muñoz, M. and Vaca, L. (2001). Functional expression of recombinant type 1 ryanodine receptor in insect sf21 cells. *Cell Calcium* **30**, 9-17.

Bootman, M. D., Lipp, P. and Berridge, M. J. (2001). The organization and functions of local Ca^{2+} signales. *J Cell Sci.* **114**, 2213-2222.

Brandl, C. J., de León, S., Martín, D. R. and MacLennan, D. H. (1987). Adult forms of the Ca^{2+}-ATPase of sarcoplasmic reticulum. Expression in developing skeletal muscle. *J. Biol. Chem.* **262**, 3768-3774.

Butanda-Ochoa, A., Höjer, G., Díaz-Muñoz, M. (2003). Modulation of the skeletal muscle Ca^{2+} release channel/ryanodine receptor by adenosine and its metabolites. A structure-activity approach. *Bioorg. Med. Chem.* (in press).

Campos-Ortega, J. A. and Hartenstein, V. (1997). *The Embryonic Development of Drosophila melanogaster*. New York: Springer-Verlag.

Cancela, J. M. (2001). Specific Ca^{2+} signaling evoked by cholecystokinin and acethylcholine: the roles of NAADP, cADPR, and IP_3. *Annu. Rev. Physiol.* **63**, 99-117.

Carafoli, E. and Klee, C. (1999). *Calcium as a Cellular Regulator*. New York: Oxford University Press.

Carafoli, E., Santella, L., Branca, D. and Brini, M. (2001). Generation, control, and processing of cellular calcium signals. *Crit. Rev. Biochem. Mol. Biol*. **36**, 107-260.

Chu, A., Dickson, M. C., Saito, A., Seiler, S. and Fleischer, S. (1988). Isolation of sarcoplasmic reticulum fractions referable to longitudinal tubules and junctional terminal cisternae from rabbit skeletal muscle. *Methods Enzymol*. **157**, 36-46.

Chu, A., Díaz-Muñoz, M., Hawkes, M. J., Brush, K. and Hamilton, S. L. (1990). Ryanodine as a probe for the functional state of the skeletal muscle sarcoplasmic reticulum calcium release channel. *Mol. Pharmacol*. **37**, 735-741.

Cifuentes, F., González, C. E., Fiordelisio, T., Guerrero, G., Lai, F. A. and Hernández-Cruz, A. (2001). A ryanodine fluorescent derivative reveals the presence of high-affinity ryanodine binding sites in the Golgi complex of rat sympathetic neurons, with possible functional roles in intracellular Ca^{2+} signaling. *Cell Signal*. **13**, 353-362.

Correa, V., Riley, A. M., Shuto, S., Horne, G., Nerou, E. P., Marwood, R. D., Potter, B. L. and Taylor, C. W. (2001). Structural determinants of adenophostin A activity at inositol trisphosphate receptors. *Mol. Pharmacol*. **59**, 1206-1215

Damiani, E., Tobaldin, G., Volpe, P. and Margreth, A. (1991). Quantitation of ryanodine receptor of rabbit skeletal muscle, heart and brain. *Biochem. Biophys. Res. Commun.* **175**, 858-865.

Deshpande, M., Venkatesh, K., Rodrigues, V. and Hasan, G. (2000). The inositol 1,4,5-trisphosphate receptor is required for maintenance of olfactory adaptation in *Drosophila* antennae. *J. Neurobiol.* **43**, 282-288.

Diaz-Muñoz, M., Dent, M. A. R., Granados-Fuentes, D., May, A. C., Hernández-Cruz, A., Harrington, M. E. and Aguilar-Roblero, R. (1999). Circadian modulation of ryanodine receptor type 2 in the SCN of rodents. *Neuroreport* **10**, 1-6.

Du, G. G., Imredy, J. P. and MacLennan, D. H. (1998). Characterization of recombinant rabbit cardiac and skeletal muscle Ca^{2+} release channels (ryanodine receptors) with a novel [^{3}H]-ryanodine binding assay. *J. Biol. Chem.* **273**, 33259-33266.

Favero, T. G. and Abramson, J. J. (1994). Thapsigargin-induced Ca^{2+} release from sarcoplasmic reticulum and asolectin vesicles. *Cell Calcium* **15**, 183-189.

Felsenstein, J. (1996). Inferring phylogenies from protein sequences by parsimony, distance, and likelihood methods. *Methods Enzymol.* **266**, 418-427.

Franck, J. P. C., Morrissette, J., Keen, J. E., Londraville, R. L., Beamsley, M. and Block, B. A. (1998). Cloning and characterization of fiber type-specific ryanodine receptor isoforms in skeletal muscles of fish. *Am. J. Physiol.* **275**, C401-C415.

Fricke, U. (1975). Tritosol: a new scintillation cocktail based on Triton X-100. *Anal. Biochem.* **63**, 555-558.

Furuichi, T., Simon-Chazottes, D., Fujino, I., Yamada, N., Hasegawa, M.,

Miyawaki, A., Yoshikawa, S., Guénet, J. L. and Mokoshiba, K. (1993). Widespread expression of inositol 1,4,5-trisphosphate receptor type 1 gene (Insp3r1) in the mouse central nervous system. *Receptors Channels* **1**, 11-24.

Gafni, J., Munsch, J. A., Lam, T. H., Catlin, M. C., Costa, L. G., Molinski, T. F. and Pessah, I. N. (1997). Xestospongins: Potent membrane permeable blockers of the inositol 1,4,5-trisphosphate receptor. *Neuron* **19**, 723-733.

Galtier, N., Gouy, M. and Gautier, C. (1996). SEAVIEW and PHYLO_WIN, two graphic tools for sequence alignment and molecular phylogeny. *Comput. Appl. Biosci.* **12**, 543-548.

Hasan, G. and Rosbash, M. (1992). *Drosophila* homologs of two mammalian intracellular Ca^{2+}- release channels: identification and expression patterns of the inositol 1,4,5-triphosphate and the ryanodine receptor genes. *Development* **116**, 967-975.

Hillis, D. M. (1991). *Discriminating between phylogenetic signal and random noise in DNA sequences* (ed. M. Miyamoto and J. Cracraft), pp. 278-294. New York: Oxford University Press.

Holmberg, S. R. M. and Williams, A. J. (1990). The cardiac sarcoplasmic reticulum-release channel: modulation of ryanodine binding and single-channel activity. *Biochem. Biophys. Acta* **1022**, 187-219.

Kukkonen, J. P., Lund, P. E. and Akerman, K. E. (2001). 2-Aminoethoxydiphenyl borate reveals heterogeneity in receptor-activated Ca^{2+} discharge and store-operated Ca^{2+} influx. *Cell Calcium* **30**, 117-129.

Lowry, O. H., Rosebrough, N. L., Farr, A. L. and Randall, R. J. (1951). Protein measurement with the Folin phenol reagent. *J. Biol. Chem.* **193**, 265-275.

MacLennan, D. H. (1990). Molecular tools to elucidate problems in excitation-contraction coupling. *Biophys. J.* **58**, 1355-1365.

MacLennan, D. H., Rice, W. J. and Green, N. M. (1997). The mechanism of Ca^{2+} transport by sarco(endo)plasmic reticulum Ca^{2+}-ATPases. *J. Biol. Chem.* **272**, 28815-28818.

Magyar, A., Bakos, E. and Varadi, A. (1995). Structure and tissue-specific expression of the Drosophila melanogaster organellar-type Ca^{2+}-ATPase gene. *Biochem. J.* **310**, 757-763.

Manunta, M., Rossi, D., Simeón, I., Butelli, E., Romanin, C., Sorrentino, V. and Schindler, H. (2000). ATP-induced activation of expressed RyR3 at low free calcium. *FEBS Lett.* **471**, 256-260.

Marks, A. R. (1997). Intracellular calcium-release channels: regulators of cell life and death. *Am. J. Physiol.* **272**, H597-H605.

Martínez-Merlos, T., Cañedo-Merino, R. and Díaz-Muñoz, M. (1997). Ryanodine receptor binding constants in skeletal muscle, heart, brain and liver of the Mexican volcano mouse (Neotomodon alstoni alstoni; Rodentia:Cricetidae). Comparison with five other rodent species. *Int. J. Biochem. Cell Biol.* **29**, 529-539.

Maryon, E. B., Coronado, R. and Anderson, P. (1996). unc-68 encodes a ryanodine receptor involved in regulating C. elegans body-wall muscle contraction. *J. Cell Biol.* **134**, 885-893.

McPherson, P. S. and Campbell, K. P. (1990). Solubilization and biochemical characterization of the high affinity [^{3}H]ryanodine receptor from rabbit brain membranes. *J. Biol. Chem.* **265**, 18454-18460.

Mikoshiba, K., Furiuchi, T. and Miyawaki, A. (1994). Structure and function of IP_3 receptors. *Semin. Cell Biol.* **5**, 273-281.

Mintz, E. and Guillian, F. (1997). Ca^{2+} transport by the sarcoplasmic reticulum ATPase. *Biochim. Biophys. Acta* **1318**, 52-70.

Misquitta, C. M., Sing, A. and Grover, A. K. (1999). Control of sarcoplasmic/endoplasmic reticulum Ca^{2+} pump expression in cardiac and smooth muscle. *Biochem. J.* **338**, 167-173.

Murayama, T., Oba, T., Katayama, E., Oyamada, H., Oguchi, K., Kobayashi, M., Otzuka, K. and Ogawa, Y. (1999). Further characterization of the type 3 rynodine receptor (RyR 3) purified from rabbit diaphragm. *J. Biol. Chem.* **274**, 17297-17308.

Nori, A., Villa, A., Podini, P., Witcher, D. R. and Volpe, P. (1993). Intracellular Ca^{2+} stores of rat cerebellum: heterogeneity within and distinction from endoplasmic reticulum. *Biochem. J.* **291**, 199-204.

Odermatt, A., Taschner, P. E. M., Khanna, V. K., Busch, H. F. M., Karpati, G., Jablecki, C. K., Breuning, M. H. and MacLennan, D. H. (1996). Mutations in the gene-encoding SERCA1, the fast-twitch skeletal muscle sarcoplasmic reticulum Ca^{2+} ATPase are associated with Broad disease. *Nat. Genet.* **14**, 191-194.

Page, R. D. M. (1996). TREEVIEW: An application to display phylogenetic trees on personal computers. *Comp. Applic. Biosci.* **12**, 357-358.

Pessah, I. N., Stambuck, R. A. and Casida, J. E. (1987). Ca^{2+}-activated ryanodine binding: mechanisms of sensitivity and intensity modulation by Mg^{2+}, caffeine, and adenine nucleotides. *Mol. Pharmacol.* **31**, 232-238.

Petersen, O. H. and Cancela, J. M. (1999). New Ca^{2+}-releasing messengers: are they important in the nervous system? *Trends Neurosci.* **22**, 488-494.

Plesner, L. (1995). Ecto-ATPases: identities and functions. *Int. Rev. Cytol.* **158**, 141-214.

Pozzan, T., Rizzuto, R., Volpe, P. and Maldolesi, J. (1994). Molecular and cellular physiology of intracellular calcium stores. *Physiol. Rev.* **74**, 595-636.

Raghu, P. and Hasan, G. (1995). The inositol 1,4,5-triphosphate receptor expression in Drosophila suggests a role for IP_3 signalling in muscle development and adult chemosensory functions. *Dev. Biol.* **171**, 564-577.

Rubtsov, A. M. and Batrukova, M. A. (1997). Histidine-containing dipeptides as endogenous regulators of the activity of sarcoplasmic reticulum Ca^{2+}-release channels. *Biochim. Biophys Acta* **1324**, 142-150.

Saborido, A., Delgado, J. and Megías, A. (1999). Measurement of sarcoplasmic reticulum Ca^{2+}-ATPase activity and E-type Mg^{2+}-ATPase activity in rat heart homogenates. *Anal. Biochem.* **268**, 79-88.

Schoenmakers, T. J., Visser, G. J., Flik, G. and Theuvenet, A. P. (1992). CHELATOR: an improved method for computing metal ion concentrations in physiological solutions. *Biotechniques* **12**, 870-879.

Sinha, M. and Hasan, G. (1999). Sequencing and exon mapping of the inositol 1,4,5-trisphosphate receptor cDNA from Drosophila embryos suggests the presence of differentially regulated forms of RNA and protein. *Gene* **233**, 271-276.

Sorrentino, V., Barone, V. and Rossi, D. (2000). Intracellular Ca^{2+} release channels in evolution. *Curr. Opin. Gen. Dev.* **10**, 662-667.

Sullivan, K. M., Scott, K., Zuker, C. S. and Rubin, G. M. (2000). The ryanodine receptor is essential for larval development in *Drosophila melanogaster*. *Proc. Natl. Acad. Sci. USA* **23**, 5942-5947.

Swatton, J. E., Morris, S. A., Wissing, F. and Taylor, C. W. (2001). Functional properties of *Drosophila* inositol trisphosphate receptors. *Biochem. J.* **359**, 435-441.

Takeshima, H., Nishi, M., Iwabe, N., Miyata, T., Hosoya, T., Masai, I. and Hotta, Y. (1994). Isolation and characterization of a gene for a ryanodine receptor/calcium release channel from *Drosophila melanogaster*. *FEBS Lett.* **337**, 81-87.

Tatusova, T. and Madden, T. L. (1999). Blast 2 sequences. A new tool for comparing protein and nucleotide sequences. *FEMS Microbiol. Lett.* **174**, 247-250.

Thompson, J. D., Gibson, T. J., Plewniak, F., Jeanmougin, F. and Higgins, D. G. (1997). CLUSTAL W: Improving the sensitivity of progressive multiple sequence alignment through sequence weighting, position specific gap penalties and weight matrix choice. *Nucleic Acids Res.* **24**, 4876-4882.

Zarka, A. and Shashan-Barmatz, V. (1993). Characterization and photoaffinity labeling of the ATP binding site of the ryanodine receptor from skeletal muscle. *Eur. J. Pharmacol.* **213**, 147-153.

Zhang, J. J., Williams, A. J. and Sitsapesan, R. (1999). Evidence for novel caffeine and Ca^{2+} binding sites on the lobster skeletal ryanodine receptor. *Br. J. Pharmacol.* **126**, 1066-1074.

Zhao, F., Li, P., Chen, S. R., Louis, C. F. and Fruen, B. R. (2001). Dantrolene inhibition of ryanodine receptor Ca^{2+} release channels. Molecular mechanism and isoform selectivity. *J. Biol. Chem.* **276**, 13810-13816.